FACTA UNIVERSITATIS
Series: **Architecture and Civil Engineering** Vol. 20, Nº 1, 2022, pp. 1-14
https://doi.org/10.2298/FUACE220421001Z

Original scientific paper

ANALYTICAL PREDICTION OF MECHANICAL PROPERTIES IN HORIZONTAL DIRECTION OF LEAD-RUBBER BEARINGS

UDC 624.042.7:550.34.01/.016

Andrija Zorić, Marina Trajković-Milenković, Dragan Zlatkov, Žarko Petrović, Todor Vacev

Faculty of Civil Engineering and Architecture, University of Niš, Serbia

Abstract. *Application of seismic isolation devices is an efficient way for designing seismically resistant structures. For that purpose, various types of seismic isolation devices are developed. The main differences between them are in the materials used for their production and in the way they provide horizontal flexibility. Dynamic analysis of a base isolated structure requires an adequate mathematical model of the seismic isolation devices which can describe their mechanical properties in horizontal and vertical directions. The paper is considering analytical models used for the prediction of mechanical properties in the horizontal direction of lead-rubber bearings, which are proposed in the contemporary literature. Results obtained using these analytical formulas are compared with the results obtained by the finite element analysis model developed in this paper, as well as with available test results provided by the manufacturer. Improvements of the existing analytical models are suggested in order to enable a better prediction of mechanical characteristics in the horizontal direction of lead-rubber bearings.*

Key words: *lead-rubber bearing, elastic stiffness, post-elastic stiffness, yield force, equivalent viscose damping ratio, finite element analysis*

1. INTRODUCTION

In seismically active areas, the effect of an earthquake on a structure is dominant in structural design. During an earthquake, damage of the structural and non-structural elements can occur, and that could also lead to the total collapse of the structure. That is the reason why the seismic protection of buildings is a very important field of research nowadays.

Received April 21, 2022 / Accepted June 7, 2022
Corresponding author: Andrija Zorić
Faculty of Civil Engineering and Architecture, Aleksandra Medvedeva 14, 18106 Niš, Serbia
E-mail: andrija.zoric@gaf.ni.ac.rs

The concept of the design of the seismically resistant structures dates back to the end of the 19th and the beginning of the 20th century, with the registration of the first patents [1, 2]. The modern base isolation concept is based on the application of the special devices mounted in the seismic dilatation. The seismic dilatation divides a structure into the isolated structure (or superstructure) and the substructure. The seismic isolation devices possess small stiffness in horizontal directions which provides an increase of the natural period of vibration and a decrease of the intensity of seismic forces in the structure compared to the rigidly founded structure. On the other hand, seismic isolation devices are stiff enough in the vertical direction to transfer the gravity load.

From the aspect of the used materials and mechanism of functioning, seismic isolators can be divided into elastomeric, sliding and combined bearings [3]. Elastomeric bearings provide the seismic isolation of structures through the flexibility of the rubber material used for their manufacture. Regarding the damping level there are low damping rubber bearings, lead-rubber bearings and high damping rubber bearings [4-7].

The lead-rubber bearings (LRB) are developed with the aim to increase the damping of the elastomeric bearings. By increasing the damping of the seismic isolation devices, the displacements of the isolated structure are reduced [8]. LRB consists of steel mounting plates, rubber, steel shims and a lead core (Fig. 1). The lead core is dominantly deformed by the shear, characterized by relatively small yield strength, and consequently by the low value of yield shear strength. Seismic energy is absorbed due to the plastic deformations of the lead core.

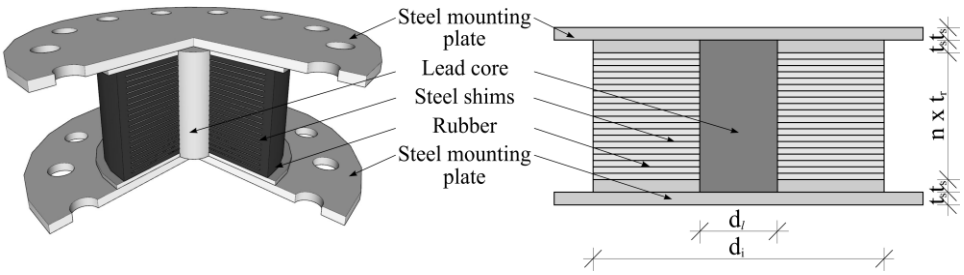

Fig. 1 The lead-rubber bearing

Mechanical characteristics of LRB are determined experimentally, and it is confirmed that the lead core provides an adequate level of seismic energy dissipation. The force-displacement relationship of LRB in the horizontal direction can be idealized by a bilinear diagram [4, 8-15]. The numerical analysis of performances of LRB is also the subject of research [16-19]. It is confirmed that the application of LRB brings benefits, as in the response of buildings [20-23], as well as in the response of bridges [24, 25], during an earthquake.

The paper analyses the nowadays widely used analytical models for prediction of the mechanical properties in the horizontal direction of LRB. Results obtained using existing analytical models are compared to the results obtained by the finite element analysis model developed in this paper and to available test results provided by the manufacturer. The analysis includes the influence of the lead core diameter on the mechanical properties in the horizontal direction of LRB, as well as the influence of the number and thickness

of the rubber layers and the number of the steel shims. Based on the comparative study of the analytical and numerical results, the calibration of the existing analytical models is performed. As a result, an improved analytical model is proposed, which exhibited a better prediction of mechanical characteristics in the horizontal direction of LRB, used for the dynamic analysis of the base isolated structures.

2. ANALYTICAL MODEL

An idealized bilinear force-displacement relationship in the horizontal direction of LRB can be defined by the elastic stiffness (K_e), post-elastic stiffness (K_y) and yield force (Q_y) (Fig. 2). The analytical relations presented in the following text are proposed in literature in order to determine the post-elastic stiffness and the yield force of LRB.

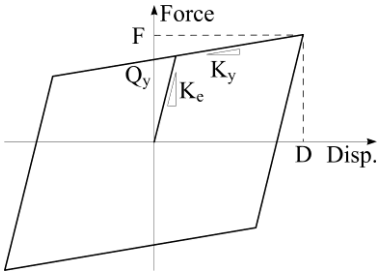

Fig. 2 Idealized bilinear force-displacement relationship in horizontal direction of LRB

The post-elastic stiffness (K_y) is defined as a superposition of stiffnesses of the elastomeric part and the lead core of LRB [6, 26]:

$$K_y = C_{Ky}\left(\frac{G_r A_r}{H} + \frac{G_l A_l}{H}\right), \tag{1}$$

where: C_{ky} – modification modulus,
G_r, G_l – shear modulus of rubber/lead,
A_r, A_l – cross-section area of laminated rubber/lead core,
H – total rubber thickness and height of lead core.

The post-elastic stiffness of LRB is dependent on the shear strain (γ) and the latter is introduced by a modification modulus C_{Ky} [6, 26]:

$$C_{Ky} = \begin{cases} 0.779\gamma^{-0.43} & (\gamma < 0.25) \\ \gamma^{-0.25} & (0.25 \le \gamma < 1.00) \\ \gamma^{-0.12} & (1.00 \le \gamma < 2.50) \end{cases}. \tag{2}$$

The other recommendation for the prediction of the post-elastic stiffness is given in [27] in the following form:

$$K_y = \left(1+12\frac{A_l}{A_r}\right)\frac{G_r A_r}{H}. \tag{3}$$

In the latest research it is noticed that the contribution of the stiffness of the lead core to the overall post-elastic stiffness of LRB is small. Therefore, a new analytical model is proposed [28]. According to this recommendation, the post-elastic stiffness of LRB is proportional to the stiffness of the elastomeric part, whereas the influence of the lead core is encompassed by the factor f, and the overall post-elastic stiffness of LRB can be calculated by the following formula:

$$K_y = f \cdot \frac{G_r A_r}{H} = 1.1 \cdot \frac{G_r A_r}{H}. \tag{4}$$

The yield force (Q_y) of LRB is proportional to the cross-sectional area of the lead core and the yield shear stress of lead (f_{yl}), while the influence of the shear strain is encompassed by a modification modulus C_{Qy} [6, 26]:

$$Q_y = C_{Qy} f_{yl} A_l, \tag{5}$$

$$C_{Qy} = \begin{cases} 2.036\gamma^{0.41} & (\gamma < 0.10) \\ 1.106\gamma^{0.145} & (0.10 \le \gamma < 0.50) \\ 1 & (\gamma > 0.50) \end{cases}. \tag{6}$$

An analytical formula for the prediction of the elastic stiffness of LRB has not been proposed yet. However, the adoption of the elastic stiffness which equals to the product of the factor β and the post-elastic stiffness (K_y) is recommended by the manufacturer of these isolation devices [29] and the other researchers [5, 27, 28], with different suggestions for the value of the factor β (6.5 or 10).

An equivalent viscose damping ratio (ξ_{eq}) is a parameter important for the estimation and modelling of the damping. The equivalent viscose damping ratio is a ratio of the total dissipated energy per cycle, which is equal to the area of the hysteretic loop (E_D), and the elastic strain energy (E_s). As a function of the maximum displacement (D) and the corresponding force (F) it can be calculated as:

$$\xi_{eq} = \frac{E_D}{4\pi E_S} = \frac{E_D}{2\pi FD}. \tag{7}$$

The equivalent viscose damping ratio of LRB can be calculated based on the mechanical properties in the horizontal direction as [6, 26]:

$$\xi_{eq} = \frac{2}{\pi}\frac{Q_y\left[\gamma H - \dfrac{Q_y}{(\beta-1)K_y}\right]}{\left(\dfrac{Q_y}{\gamma H}+K_y\right)(\gamma H)^2}. \tag{8}$$

3. NUMERICAL ANALYSIS

For the purpose of calibration of the existing analytical models, a numerical analysis of the mechanical characteristics in the horizontal direction of LRB has been conducted by the finite element analysis using the software package Ansys Workbench. For the numerical analysis, LRB with the isolator diameter d_i = 650 mm (Fig. 1), produced by the manufacturer Dynamic Isolation Systems [29], is chosen. The influence of the lead core diameter (d_l) on the mechanical properties of LRB is analysed for the cases of d_l = 50, 100, 150 and 200 mm. In order to obtain the impact of the number of rubber layers on the mechanical properties of LRB, two types of isolators are examined in the numerical analysis. The first type of isolators is composed of n = 20 layers of t_r = 12 mm thick rubber whereas the second is composed of n = 10 layers of t_r = 24 mm thick rubber. Steel shims 3 mm thick are between the rubber layers. On the top and bottom of the isolator are two steel plates with thickness t_s = 32 mm. All these variants provided eight different models for analysis, systematized in Table 1.

Table 1 Analysed models

Name	Lead core diameter d_l [mm]	Number of rubber layers n	Rubber layer thickness t_r
D50N20	50	20	12
D100N20	100		
D150N20	150		
D200N20	200		
D50N10	50	10	24
D100N10	100		
D150N10	150		
D200N10	200		

3.1. Geometry, material models and finite element mesh

The geometry of the models is developed in accordance to the adopted geometry of the analysed models. The geometry and loads are symmetric in regard to the middle vertical plane, therefore only one half of the isolator is modelled with the aim to decrease the number of finite elements and to rationalize the numerical calculation. Steel mounting plates are not modelled because their influence on the mechanical properties of LRB is negligible. The geometry of the models D150N20 and D150N10 is shown in Fig. 3. The geometry of the other models is similar except for the different lead core diameter.

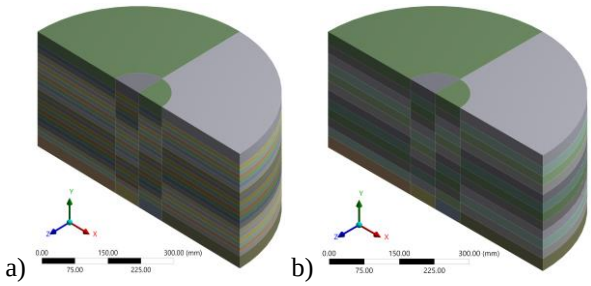

Fig. 3 Geometry of the numerical models: a) D150N20, b) D150N10

Nonlinear characteristics of the steel parts are modelled with the bilinear kinematic material model. The modulus of elasticity of steel is E = 200 GPa and Poisson's ratio is $\nu = 0.30$. Linear elastic behaviour of steel is up to the yield stress $f_y = 250$ MPa, after which the plastic deformations occur (Fig. 4a). In the plastic regime, the stress is proportional to the strain by the tangent modulus $E_t = 1450$ MPa. Nonlinear characteristics of the lead are modelled with the bilinear isotropic material model, where the modulus of elasticity is E = 17500 MPa, Poisson's ratio $\nu = 0.44$, and the yield stress is $f_y = 10$ MPa. In the plastic regime there is no hardening, i.e., the tangent modulus is equal to zero (Fig. 4b). The rubber is a hyperelastic material, modelled by the Neo-Hookean material model with the initial shear modulus $\mu_0 = 0.40$ MPa and an incompressibility parameter $d = 0.001$ MPa^{-1} defined for the typically assumed bulk modulus of rubber 2000 MPa [30].

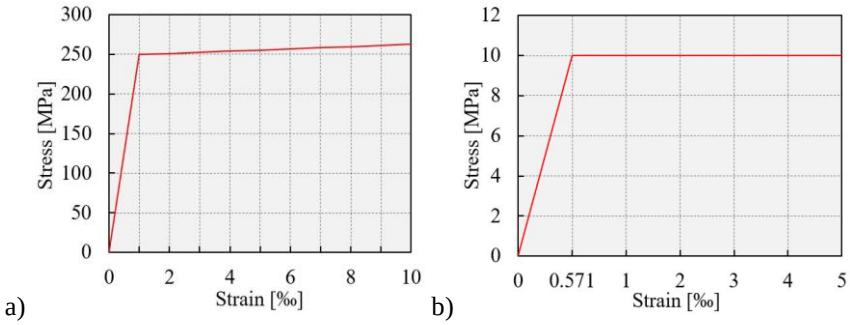

Fig. 4 Stress-strain diagram: a) steel, b) lead

The solid finite element with 20 nodes and three translational degrees of freedom (DOF) per node (SOLID186) is adopted for steel plates, lead core and rubber. This finite element is suitable for modelling the elastoplastic and hyperelastic behaviour of material, as well as for modelling the geometric nonlinearity [31]. For the steel shims the shell finite element with 8 nodes and three translational and three rotational DOF per node (SHELL281) is adopted. This finite element is suitable for modelling steel shims including their material and geometric nonlinear behaviour [31]. The finite element mesh is rotationally symmetric, which corresponds to the symmetry of the geometry. The nodes of the rubber, steel shims and lead core in the zone of contact are merged. Therefore, the interaction of these parts is modelled as discrete, without sliding, friction and separation, which is an idealisation of the problem with the aim of simplifying the numerical models. The finite element mesh density in all analysed models is similar. However, there are differences in the number of finite elements and nodes due to the differences in the geometry. The number of finite elements is in the range of 5664 to 6464 in the models with 20 layers of 12 mm thick rubber, and the number of nodes is in the range of 15314 to 18235. In the models with 10 layers of 24 mm thick rubber the number of finite elements is in the range of 2936 to 3504, and the number of nodes is in the range of 9597 to 10865. The finite element mesh of the models D150N20 and D150N10 is shown in Fig. 5. The finite element mesh of the other models is similar except for the different lead core diameter.

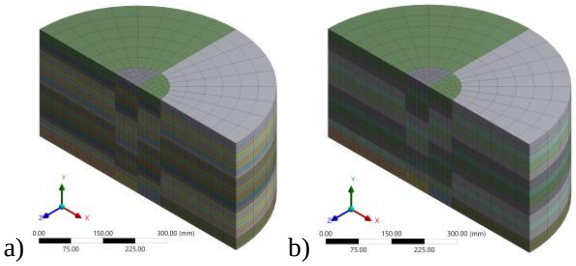

Fig. 5 Finite element mesh: a) D150N20, b) D150N10

3.2. Boundary conditions and loads

The seismic isolation device is placed on a substructure, so all translations of the bottom surface of the isolator are constrained (Fig. 6a). The upper surface of the isolator is connected to the isolated superstructure, so the translation of the surface is allowed, but the rotations are constrained, which is modelled by applying the appropriate boundary conditions (Fig. 6b). Due to the symmetry of the geometry only one half of the isolator was modelled and the influence of the other half is included by defining a symmetry boundary condition on the vertical symmetry plane (Fig. 6c).

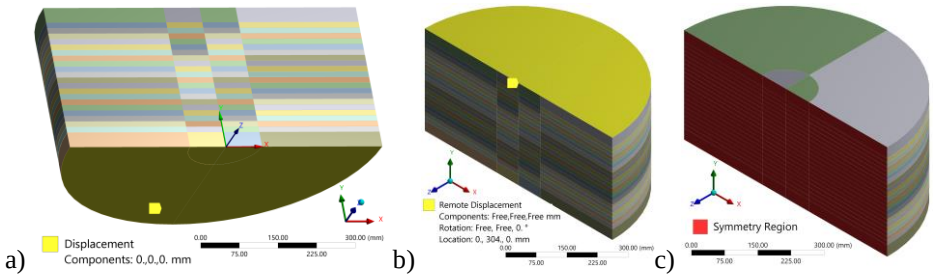

Fig. 6 Boundary conditions: a) support at the lower surface of LRB, b) fixed rotation around z axis at the top surface of LRB, c) symmetry boundary condition

The seismic isolation device is loaded by the gravity load of the isolated superstructure. In the numerical analysis the vertical load was applied as 4 mm displacement of the upper surface of the isolator in the vertical direction (Fig. 7a). The vertical displacement is defined in the first step of the analysis and kept constant in all further steps in which the horizontal load is acting. For the analysed LRB the maximum declared displacement in the horizontal direction is 410 mm [29]. In the numerical analysis of the force-displacement relationship the horizontal displacement is defined in the x direction (Fig. 7b). In the first step of the analysis, when only the vertical displacement is applied, the horizontal displacement is equal to zero, while during the last three steps the full cycle of horizontal displacement with magnitude ±400 mm is applied (Fig. 7c).

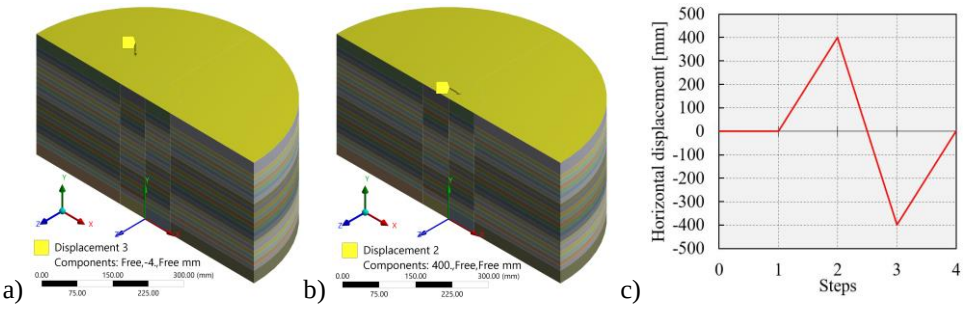

Fig. 7 Loads: a) vertical displacement, b) horizontal displacement, c) rate of horizontal displacement

3.3. Analysis parameters

The numerical analysis includes material and geometric nonlinearity. In order to obtain convergence of the calculation it is necessary to apply load in small increments. Consequently, each analysis step is initially divided into 1600 substeps, while the minimum and maximum number of substeps are 400 and 16000, respectively. Force, displacement and moment convergence criteria are set by the software package. As output results, force-displacement relationship and a von-Mises stress for evaluation of plastification of the lead core are chosen.

3.4. Numerical results

The force-displacement relationship in the horizontal direction, for all analysed models, is shown in Fig. 8. The results are presented as a comparative analysis of the

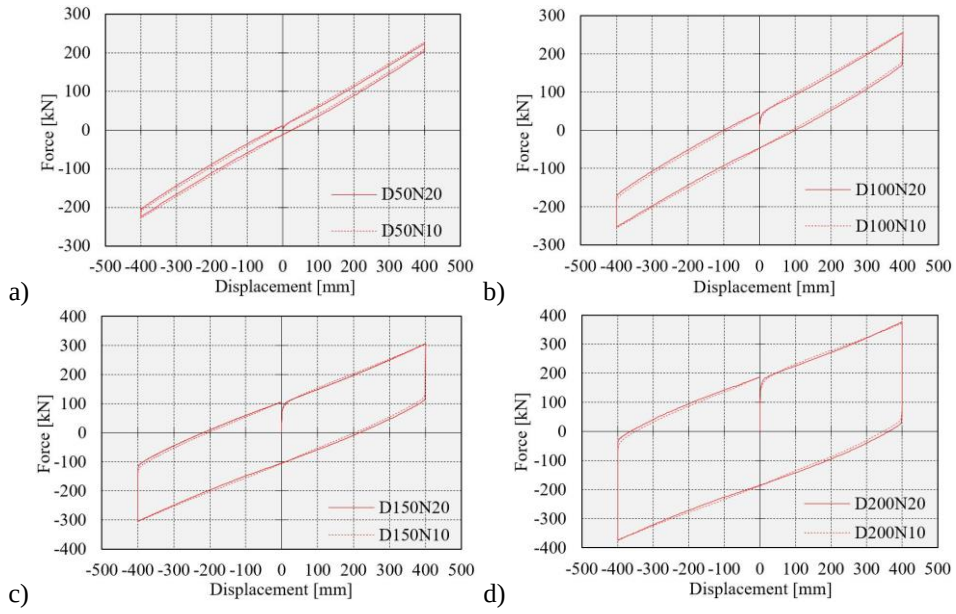

Fig. 8 Force-displacement relationship in horizontal direction: a) D50N20 and D50N10, b) D100N20 and D100N10, c) D150N20 and D150N10, d) D200N20 and D200N10

influence of the number and thickness of rubber layers. It can be concluded that the difference between hysteretic loops, in cases of different number and thickness of rubber layers, is negligible. This result confirms analytical formulas presented in Section 2 from the aspect that the number and thickness of rubber layers and number of steel shims do not influence the mechanical properties in the horizontal direction of LRB.

The area of hysteretic loops as a measure of the dissipated energy is proportional to the diameter of the lead core. Due to the low yield stress of lead, the plastic deformation of the lead core occurs at small horizontal displacement of the isolator, so the lead core is fully plastified under considered cyclic horizontal displacements (Fig. 9).

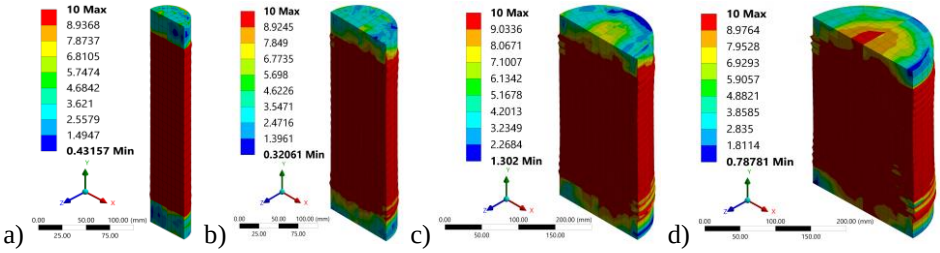

Fig. 9 Von-Mises stress of lead core: a) D50N20, b) D100N20, c) D150N20, d) D200N20

The post-elastic stiffness, the yield force and the equivalent viscose damping ratio are calculated based on the numerical results. The comparative analysis of the numerical and analytical results and the calibration of the analytical models are performed in the next section.

4. Calibration of the Analytical Models

4.1. Post-elastic stiffness

Based on the Eqs. (1), (3) and (4), the post-elastic stiffness is calculated for different cases of the diameter of the lead core of LRB. Results are systematized and compared with the numerical results (see Table 2).

Table 2 The post-elastic stiffness according to the numerical analysis and the existing analytical models

Lead core diameter d_l [mm]	Post-elastic stiffness [kN/m]			
	Numerical analysis	Analytical model, equation (1)	Analytical model, equation (3)	Analytical model, equation (4)
50	550.37	47273.63	589.05	604.76
100	541.46	187534.01	697.04	593.96
150	524.52	421301.32	877.03	575.96
200	505.37	748575.55	1129.01	550.76

From the Table 2, it can be concluded that the existing analytical model based on Eq. (1) overestimates the post-elastic stiffness. Better results are obtained by the analytical

model based on Eq. (3), but in the case of a large diameter of the lead core, the post-elastic stiffness starts to increase significantly over the experimentally obtained range [29]. This is a consequence of taking into account the stiffness of the lead core in the existing analytical models. The analytical model based on Eq. (4) gives a better prediction of the post-elastic stiffness than the other two models, since the difference between the analytical and numerical results is around 10 %.

In this paper, a new analytical model is proposed. Namely, as it is stated in Section 3.4, the total plastification of the lead core occurs at relatively small displacements. Therefore, as a result of the analysis, it can be recommended that only the stiffness of the elastomeric part should be accounted for in the post-elastic stiffness of LRB. The stiffness of the lead core should be neglected, since, it does not contribute to the post-elastic stiffness of LRB after the total plastification. This means that the post-elastic stiffness of LRB should be calculated using the following relation:

$$K_y = C_{Ky} \frac{G_r A_r}{H}. \tag{9}$$

The post-elastic stiffness, calculated by the newly proposed Eq. (9), is compared with the obtained numerical results (see Fig. 10). It can be concluded that the proposed analytical model correctly predicts the post-elastic stiffness of LRB for all cases of the lead core diameter since the differences between the analytical and numerical results are less than 7 %. Also, the post-elastic stiffnesses calculated by the proposed Eq. (9) is in a very good correlation to the experimental results given by the manufacturer [29].

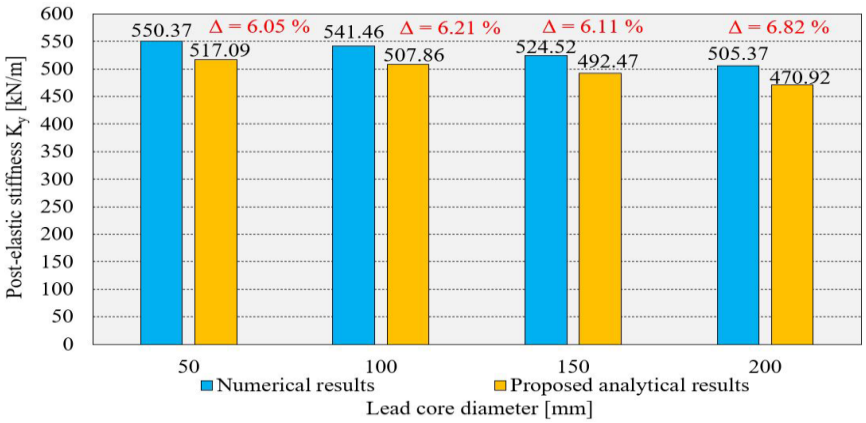

Fig. 10 Comparison of the numerical and proposed analytical results of the post-elastic stiffness

4.2. Yield force

Determining the yield force using Eq. (5) requires defining of the yield shear stress of lead (f_{yl}). This quantity usually cannot be easily defined, so one can use the more available quantity, the yield stress (f_y), which is equal to 10 MPa in the analysed models. In order to determine the yield shear stress, the von Mises or Tresca yield criterion can be applied. According to the von Mises criterion, the yield shear stress is 57.74 % of the yield stress, while according to the Tresca criterion it is 50 % [32]. With such defined

values of the yield shear stress, the yield force was calculated for different cases of the diameter of the lead core of LRB. The results are summarized and compared to the numerical results (see Fig. 11). It can be concluded that the von Mises criterion for the definition of the yield shear stress gives the yield force of LRB which is in a good correlation to the numerical results, taking into account that differences between analytical and numerical results are less than 3 %, while using the Tresca criterion these differences are around 15 %.

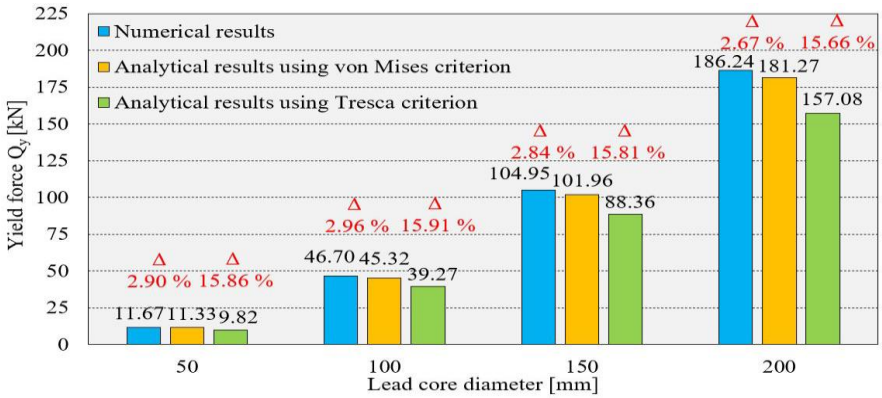

Fig. 11 Comparison of the numerical and proposed analytical results of yield force

4.3. Elastic stiffness

The elastic stiffness of LRB for the dynamic analysis of the isolated structure is defined as the post-elastic stiffness multiplied by the factor β. The equivalent viscose damping ratio of the analysed models with different lead core diameters was calculated based on the numerical results and Eq. (7) (Table 3).

Table 3 Equivalent viscose damping ratio based on the numerical analysis

Lead core diameter d_l [mm]	Equivalent viscose damping ratio ξ_{eq} [%]
50	3.23
100	11.37
150	21.36
200	30.78

From the Eq. (8), it can be concluded that the equivalent viscose damping ratio of LRB depends on the factor β. Calibration of the recommended value of the factor β is conducted based on the numerical results of the equivalent viscose damping ratio. Analytical formula Eq. (8) is used to calculate values of the equivalent viscose damping ratio of LRB for the factor β = 10, 20, 30, 40, 50, 100, ∞, and the results are shown in Fig. 12. It can be concluded that the proposed value of the factor β = 10 gives satisfying values of the equivalent viscose damping ratio for isolators with the lead core diameter up to 100 mm (difference between the numerical and analytical results is less than 2 %). In the cases of the isolators with the lead core diameter 150 mm, the authors suggest to use

the value of the factor β = 30, and in the case of the isolators with the lead core diameter 200 mm the value of the factor β = 100, in order to obtain the satisfying results for the equivalent viscose damping ratio. This conclusion comes from the comparative analysis of the analytical and numerical results.

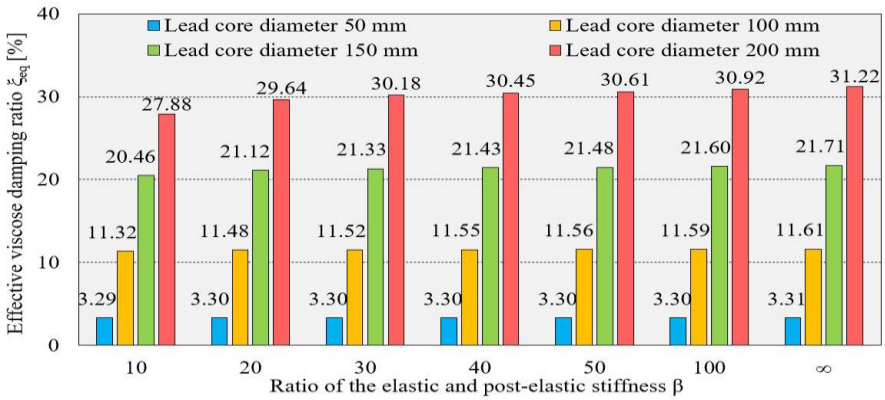

Fig. 12 The equivalent viscose damping ratio for different values of factor β

5. CONCLUSIONS

The existing analytical models for the prediction of mechanical properties in the horizontal direction of the lead-rubber bearings are presented in the paper. Based on the conducted finite element analysis of the adopted LRB isolator, with variation of the lead core diameter, number and thickness of rubber layer and number of steel shims, the calibration of the existing analytical model is performed and corrected analytical model and recommendations are given. With the newly proposed model and recommendations one can obtain a better prediction of the mechanical properties in the horizontal direction of the lead-rubber bearing. Taking into account everything presented in this paper, it can be concluded:

- The number and thickness of the rubber layers, as well as the number of steel shims, have negligible effects on the mechanical properties in the horizontal direction of the lead-rubber bearing, therefore their influence should not be included in the analytical model,
- The existing analytical models overestimate the post-elastic stiffness regarding the numerical results and experimental results given by the manufacturer,
- The post-elastic stiffness should be determined including only the stiffness of the elastomeric part of the isolator in order to obtain satisfying results,
- The value of the yield shear stress of lead is necessary in the calculation of the yield force. According to that, the application of the von Mises criterion is recommended for defining the yield shear stress based on the yield stress of lead rather than the Tresca criterion.
- The elastic stiffness is defined as the product of the post-elastic stiffness and the factor β and it is recommended to use value of 10 for the factor β for lead-rubber bearings with the lead core diameter up to 100 mm, whereas in the cases of the lead core diameter 150 mm and 200 mm, the value of 30 and 100 should be used, respectively.

The aim of this paper is to give a contribution to the more precise determination of mechanical properties in the horizontal direction of lead-rubber bearings. A better prediction of mechanical properties of lead-rubber bearings leads to a more accurate dynamic models for the analysis of response of an isolated structure during earthquakes, which is very important for the contemporary engineering practice.

Further research should be focused on development of a more accurate analytical model for prediction of the lead-rubber bearings elastic stiffness. Furthermore, the development of the numerical models of the lead-rubber bearings with different isolator diameter and comparison of the results with the new proposed analytical model would be useful for the additional validation.

REFERENCES

1. J. Touaillon, "Improvement in buildings", United States of America Patent No. 99,973, Feb. 15. 1870.
2. J. A. Calantarients, "Building construction to resist the action of earthquake", United States of America Patent No. 932,443, Aug. 31. 1909.
3. T. E. Saaed, G. Nikolakopoulos, J.-E. Jonasson and H. Hedlung, "A state-of-the-art review of structural control systems", J. Vib. Control, vol. 21, issue 5, pp. 919-937, 2015.
4. J. M. Kelly, "Aseismic base isolation: review and bibliography", Soil. Dyn. Earthq. Eng., vol. 5, issue 3, pp. 202-216, 1986.
5. F. Naeim and J. M. Kelly, Design of seismic isolated structures: from theory to practice, New York: John Wiley & Sons, 1999.
6. M. Higashino and S. Okamoto, Response Control and Seismic Isolation of Buildings, London: Taylor & Francis, 2006.
7. G. P. Warn and K. L. Ryan, "A Review of Seismic Isolation for Buildings: Historical Development and Research Needs", Buildings, vol. 2, issue 3, pp. 300-325, 2012.
8. W. H. Robinson and A. G. Tucker, "A Lead-Rubber Shear Damper", Bull. N. Z. Soc. Earthq. Eng., vol. 10, issue 3, pp. 151-153, 1977.
9. W. H. Robinson and A. G. Tucker, "Test results for lead-rubber bearings for WM. Clayton Building, Toe Toe Bridge and Waiotukupuna Bridge", Bull. N. Z. Soc. Earthq. Eng., vol. 14, issue 1, pp. 21-33, 1981.
10. W. H. Robinson, "Lead-Rubber Hysteretic Bearings Suitable for Protecting Structures during Earthquake", Earthq. Eng. Struct. Dyn., vol. 10, issue 4, pp. 593-604, 1982.
11. J. S. Hwang and J. M. Chiou, "An equivalent linear model of lead-rubber seismic isolation bearings", Eng. Struct., vol. 18, issue 7, pp. 528-536, 1996.
12. G. P. Warn and A. S. Whittaker, "A Study of the Coupled Horizontal-Vertical Behavior of Elastomeric and Lead-Rubber Seismic Isolation Bearings", Report No. MCEER-06-0011, University of Buffalo, New York, USA, 2006.
13. G. P. Warn, A. S. Whittaker and M. C. Constantinou, "Vertical Stiffness of Elastomeric and Lead-Rubber Seismic Isolation Bearings", J. Struct. Eng., vol. 133, issue 9, pp. 1227-1236, 2007.
14. S. Eem and D. Hahm, "Large strain nonlinear model of lead rubber bearings for beyond design basis earthquakes", Nucl. Eng. Technol., vol. 51, issue 2, pp. 600-606, 2019.
15. G.-H. Koo, T.-M. Shin and S.-J. Ma, "Shaking Table Tests of Lead Inserted Small-Sized Laminated Rubber Bearing for Nuclear Component Seismic Isolation", Appl. Sci., vol. 11, issue 10, pp. 1-17, 2021.
16. Y.-f. Wu, H. Wang, A.-q. Li, D.-m. Feng, B. Sha and Y.-p. Yhang, "Explicit finite element analysis and experimental verification of a sliding lead rubber bearing", J. Zhejiang Univ. Sci. A, vol. 18, issue 5, pp. 363-376, 2017.
17. M. Saedniya and S. B. Talaeitaba, "Numerical modeling of elastomeric seismic isolators for determining force-displacement curve from cyclic loading", Int. J. Adv. Struct. Eng., vol. 11, issue 3, pp. 361-376, 2019.
18. M. Trajković-Milenković, O. T. Bruhns and A. Zorić, "On instability of constitutive models for isotropic elastic-perfectly plastic material behaviour at finite deformations", J. Mech. Eng. Sci., vol. 235, issue 20, pp. 4692-4703, 2021.
19. A. Khaloo, A. Maghsoudi-Barmi and M. E. Moeini, "Numerical parametric investigation of hysteretic behavior of steel-reinforced elastomeric bearings under large shear deformation", Structures, vol. 26, pp. 456-470, 2020.

20. Y.-S. Choun, J. Park and I.-K. Choi, "Effects of Mechanical Property Variability in Lead Rubber Bearings on the Response of Seismic Isolation System for Different Ground Motions", Nucl. Eng. Technol., vol. 46, issue 5, pp. 605-618, 2014.
21. V.-T. Nguyen and X.-D. Nguyen, "Seismic response of multi-story building isolated by Lead-Rubber Bearings considering effects of the vertical stiffness and buckling behaviors", VII International Scientific Conference: Integration, Partnership and Innovation in Construction Science and Education, IOP Conference Series: Material Science and Engineering, Tashkent, Uzbekistan, 2020.
22. S.-H. Ju, C.-C. Yuantien and W.-K. Hsieh, "Study of Lead Rubber Bearing for Vibration Reduction in High-Tech Factories", Appl. Sci., vol. 10, issue 4, pp. 1-17, 2020.
23. A. Zorić, D. Zlatkov, M. Trajković-Milenković, T. Vacev and Ž. Petrović, "Analysis of seismic response of an RC frame structure with lead rubber bearings", Proceedings of 15th International Scientific Conference: Planing, Design, Construction and Renewal in the Civil Engineering iNDis 2021, University of Novi Sad, Faculty of Technical Sciences, Department of Civil Engineering and Geodesy, Novi Sad, Serbia, pp. 109-118, November 2021.
24. A. Hammed, M.-S. Koo, T.D. Do and J.-H. Jeong, "Effect of Lead Rubber Bearing Characteristics on the Response of Seismic-isolated Bridges", KSCE J. Civ. Eng., vol. 12, issue 3, pp. 187-196, 2008.
25. N. Shaban and A. Caner, "Shake table tests of a different seismic isolation systems on a large scale structure subjected to low to moderate earthquakes", J. Traffic Transp. Eng., vol. 5, issue 6, pp. 480-490, 2018.
26. T. K. Datta, Seismic Analysis of Structures, Singapore: John Wiley & Sons (Asia) Pte Ltd, 2010.
27. J. S. Hwang and L. H. Sheng, "Equivalent elastic seismic analysis of base-isolated bridges with lead-rubber bearings", Eng. Struct., vol. 16, issue 3, pp. 201-209, 1994.
28. M. L. Marsh, I. G. Buckle, E. Jr. Kavazanjian, LRFD Seismic Analysis and Design of Bridges Reference Manual, Publication No. FHWA-NHI-15-004, U.S. Department of Transportation Federal Highway Administration, Washington D.C., 2014.
29. Dynamic Isolation Systems, http://www.dis-inc.com/technical.html, accessed 10 February 2022.
30. T. Zhou, Y.-F. Wu and A.-Q. Li, "Numerical Study on the Ultimate Behavior of Elastomeric Bearings under Combined Compression and Shear", KSCE J. Civ. Eng., vol. 22, issue 9, pp. 3556-3566, 2018.
31. Ansys Software documentation. ANSYS Inc., Canonsburg, PA. 2012.
32. H. Altenbach, A. Bolchoun and V. P. Kolupaev, "Phenomenological Yield and Failure Criteria", in Plasticity of Pressure-Sensitive Materials, H. Altenbach and A. Öchsner, Eds. Berlin, Heidelberg: Springer, 2014, pp 49-152.

ANALITIČKA PREDIKCIJA MEHANIČKIH KARAKTERISTIKA U HORIZONTALNOM PRAVCU GUMENOG LEŽIŠTA SA OLOVNIM JEZGROM

Primena uređaja za seizmičku izolaciju je efikasan način za projektovanje seizmički otpornih konstrukcija. Razvijene su različite vrste uređaja za seizmičku izolaciju. Glavne razlike između njih se ogledaju u primenjenim materijalima i načinu na koji obezbeđuju horizontalnu fleksibilnost. Dinamička analiza bazno izolovanih konstrukcija zahteva adekvatan matematički model za opisivanje mehaničkih karakteristika u horizontalnom i vertikalnom pravcu uređaja za seizmičku izolaciju. U radu su analizirani analitički izrazi za predviđanje mehaničkih karakteristika u horizontalnom pravcu gumenog ležišta sa olovnim jezgrom. Rezultati dobijeni analitičkim izrazima su upoređeni sa rezultatima dobijenim na osnovu numeričkog modela metodom konačnih elemenata razvijenog u ovom radu i dostupnim rezultatima ispitivanja proizvođača. Postojeći analitički izrazi su unapređeni kako bi se adekvatnije definisale mehaničke karakteristike u horizontalnom pravcu gumenih ležajeva sa olovnim jezgrom.

Ključne reči: *gumeno ležište sa olovnim jezgrom, elastična krutost, postelastična krutost, karakteristična čvrstoća, ekvivalentno viskozno prigušenje, metod konačnih elemenata*